RESEARCH & DEVELOPMENT

Improved Estimation of Embedded Pile Length for Reuse or Pile Scour Evaluation

Murthy N. Guddati, Ph.D.
M. Shamim Rahman, Ph.D.
Vivek Samu, M.S.

Department of Civil, Construction and Environmental Engineering
North Carolina State University

Technical Report Documentation Page

1. Report No. FHWA/NC/2016-21	2. Government Accession No. *…leave blank…*	3. Recipient's Catalog No. *…leave blank…*	
4. Title and Subtitle Improved Estimation of Embedded Pile Length for Reuse or Pile Scour Evaluation		5. Report Date *April 20, 2018*	
		6. Performing Organization Code *…leave blank…*	
7. Author(s) Murthy N. Guddati, M. Shamim Rahman, Vivek Samu		8. Performing Organization Report No. *…leave blank…*	
9. Performing Organization Name and Address North Carolina State University Department of Civil Engineering Raleigh, NC 27695-7908		10. Work Unit No. (TRAIS) *…leave blank…*	
		11. Contract or Grant No. *…leave blank…*	
12. Sponsoring Agency Name and Address North Carolina Department of Transportation Research and Development Unit 104 Fayetteville Street Raleigh, North Carolina 27601		13. Type of Report and Period Covered *Final Report* *07/01/2015 to 06/30/2017*	
		14. Sponsoring Agency Code *2016-21*	
Supplementary Notes: *…leave blank…*			

16. Abstract

A longstanding threat to bridge safety is that bridge foundations can be susceptible to scour. This problem is compounded when the bridge foundation depth is unknown. According to the National Bridge Inventory, about 28,000 highway bridges with unknown foundation depths were recorded in 2016. Researchers have developed and investigated several methods over the years to determine embedded foundation lengths, including sonic echo/impulse response methods, bending wave method, various borehole methods, and many extensions and modifications of these methods. The borehole methods are considered reliable but expensive, and the surface-based methods are less expensive but lack the same level of reliability as the borehole methods. To address this problem, we have developed a new surface-based nondestructive test method that we call 'effective dispersion analysis of reflections' (EDAR). We show that EDAR is not only inexpensive, but also accurate and reliable. The method is based on accurately capturing the dispersion of waves as they propagate through a pile and is applicable to both longitudinal and bending waves. Specifically, EDAR processes measured accelerations at two distinct locations on the pile due to hammer impact, resulting in an estimate of the pile length: the analysis hinges on examining the oscillations in phase difference that are due to reflections as a function of wavenumber. We have validated EDAR using side impacts on concrete-filled steel tubes; the results consistently showed less than 5 percent error in a laboratory setting.

17. Key Words *Unknown foundation, pile, length estimation, flexural waves, reflection*	18. Distribution Statement *…leave blank…*		
19. Security Classif. (of this report) Unclassified	20. Security Classif. (of this page) Unclassified	21. No. of Pages 28	22. Price *…leave blank…*

Form DOT F 1700.7 (8-72)   **Reproduction of completed page authorized**

DISCLAIMER

The contents of this report reflect the views of the author(s) and not necessarily the views of the University. The author(s) are responsible for the facts and the accuracy of the data presented herein. The contents do not necessarily reflect the official views or policies of either the North Carolina Department of Transportation or the Federal Highway Administration at the time of publication. This report does not constitute a standard, specification, or regulation.

Acknowledgments

Executive Summary

A longstanding threat to bridge safety is that bridge foundations can be susceptible to scour. This problem is compounded when the bridge foundation depth is unknown. According to the National Bridge Inventory, about 28,000 highway bridges with unknown foundation depths were recorded in 2016. Researchers have developed and investigated several methods over the years to determine embedded foundation lengths which are broadly classified as surface-based techniques and borehole-based techniques. Surface-based techniques mainly include sonic echo/impulse response type methods and bending wave method. Several borehole-based methods which include parallel seismic, cross-hole sonic, borehole sonic, borehole radar, and borehole ultrasonic methods as well as induction testing and borehole magnetic testing for steel piles have also been developed. The borehole methods are considered reliable but expensive, and the surface-based methods are less expensive but lack the same level of reliability as the borehole methods. To address this problem, we have developed a new surface-based nondestructive test method that we call 'effective dispersion analysis of reflections' (EDAR). EDAR is not only inexpensive since it falls in the category of surface-based method, but also accurate and reliable. The method is based on accurately capturing the dispersion of waves as they propagate through a pile and is applicable to both longitudinal and bending waves. Specifically, EDAR processes measured accelerations at two distinct locations on the pile due to hammer impact, resulting in an estimate of the pile length. EDAR analysis hinges on examining the oscillations in phase difference that are due to reflections as a special function of wavenumber which is defined using the dispersion relation. The oscillations in phase difference are a consequence of the initial and reflected wave arrivals at the sensor locations and are related to the distance between the sensors and the distance from the sensor to the pile tip where the wave gets reflected. This relationship between the oscillations and the lengths is explained using simple bar and beam wave propagation theories and is used to obtain the length of the pile. We have validated EDAR using side impacts on concrete-filled steel tubes in laboratory setting. The results consistently showed less than 5 percent error in a laboratory setting.

Table of Contents

List of Figures

List of Tables

1 Introduction

Even after more than two decades of research and implementation ([1],[2],[3]), the National Bridge Inventory reports that the United States has about 28,000 bridges with unknown foundation depths in 2016 that could be potentially susceptible to scour. The scour vulnerability of a bridge cannot be determined until the embedded depth of the foundation is known, and records that contain the total lengths of piles do not always exist. Thus, in order to evaluate the potential for scour, nondestructive evaluation (NDE) techniques are needed to estimate the length of embedded piles.

One class of NDE methods for pile foundations is borehole techniques, which include parallel seismic, cross-hole sonic, borehole sonic, borehole radar, and borehole ultrasonic methods as well as induction testing and borehole magnetic testing for steel piles (see [4]–[10] for examples). All these tests require either a borehole alongside the pile foundation or a pre-installed test pipe in the pile. They also require expensive equipment along with an experienced user to interpret the results. Even though these techniques are reliable and applicable to a vast number of situations, using borehole methods to test a large group of piles is not practical due to excessive costs and site limitations.

The other class of NDE methods is surface-based techniques, which do not require drilling boreholes. These methods include sonic echo, impulse response, ultra-seismic, and bending wave (short kernel) methods. Levy [11] and Dunn [12] pioneered work that led to the development of the sonic echo and impulse response techniques. Both methods are based on generating a longitudinal wave using a hammer impact on the top of a pile and analyzing the obtained response in the time domain for the sonic echo method and in the frequency domain for the impulse response method. Specifically, in time domain length estimates are obtained by identifying peaks associated with initial and reflected waves. This methodology became more prevalent after the advent of digital signal processing, starting with the work of Rausche et al. [13].Several researchers have continued to use this methodology since then for a variety of situations [14]–[19]. Most importantly, however, using these methods when the top of the pile is inaccessible adds considerable difficulty as peak picking becomes complicated when the impact is not on the top. Recent work by Rashidyan [20] investigated sonic echo type of methods for existing timber piles without top access; however, other researchers determined that this method is not successful when testing steel H piles [21]. An extension of the sonic echo method using multiple sensors on the pile side, known as the ultra-seismic method, also has been established. All these surfaced-based methods rely on producing a wave that is dominated by longitudinal mode. However, due to the inaccessibility of the pile top, this process remains difficult because other types of waves also play a significant part in the data collected.

In order to try to solve the problems associated with an inaccessible pile top, Holt and Douglas first conceived the idea of using lateral impacts to induce flexural waves rather

than using the impact-echo method to induce conventional longitudinal waves [22]. A lateral impact imparts most of the energy into bending waves that are dispersive in nature thus, it is essential to deal with dispersive flexural waves. To this end, Holt and Douglas [22] introduced the bending wave or short kernel method to process responses from dispersive flexural waves to obtain travel-time information, which attempts to delineate the peaks through convolution, thereby enabling the application of simple travel-time algorithms. Although this idea is innovative, the choice of short kernel and subsequent peak selection is complicated, even for experienced users, resulting in subjective estimates with large errors (see e.g., [23]). Other techniques, such as Hilbert-Huang transform or continuous wavelet transform have been used by Subhani et al. [23], Farid [24] and Sheng-Hugo et al. [25]. All these techniques are based purely on signal processing and do not explicitly incorporate the underlying dispersion properties of the generated waves that could be utilized constructively to develop pile length estimation techniques.

Given both the advantages of using side impacts and the limitations associated with the existing processing techniques for flexural waves, we propose a new signal processing technique we call 'effective dispersion analysis of reflections' (EDAR). EDAR extracts length information by carefully considering the physics of wave dispersion, which has been ignored thus far in relevant methodologies. The experimental set-up for EDAR is identical to flexural wave testing, but the critical data processing step is fundamentally different and built on robust mathematical analysis that is, in turn, built on the precise dispersion relation that represent wave physics. We verified the proposed methodology using synthetic data and validated it using laboratory experiments.

The outline of the rest of the paper is as follows. Section 2 contains the problem definition and experimental set-up. A detailed derivation of the EDAR technique is given in Section 3, starting from simple longitudinal waves and leading to more complicated flexural waves. Section 4 contains the results from the laboratory validation effort, followed by conclusions in Section 5.

2 Problem Definition and Experimental Set-up

Pile foundations are long shafts made of various materials, such as timber, concrete, steel, or a combination thereof, and are either cast in place or driven deep into the soil. Many bridges have part of the pile exposed above the soil, terminating in the pile cap. The aim is to estimate the embedded length of the pile using nondestructive testing. To achieve this aim, the pile foundation is excited by imparting a sharp strike using a hand-held hammer, and the response is measured at a minimum of two locations in the foundation using sensors such as accelerometers or geophones. Depending on the location and type of excitation imparted to the pile, several types of waves can exist, such as longitudinal, flexural, and high order guided waves. Figure 1 presents a typical pile subjected to lateral impact, which is also the experimental set-up used in this study.
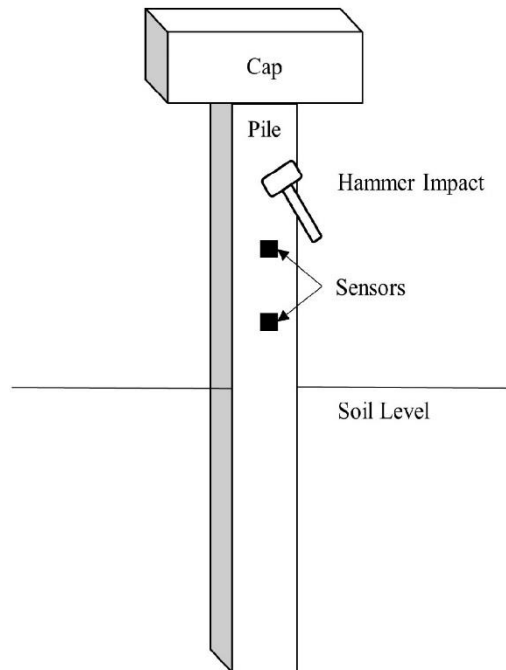
Figure 1: Pile and experimental set-up schematic.

We employed EDAR to process responses measured at two sensor locations along the length of a pile. EDAR can be applied for both longitudinal and flexural waves. Similar to the aforementioned surface-based methods, EDAR requires access to the exposed portion of the pile to record accelerations or velocity from a hammer impact at a minimum of two locations along the length of the pile. The major contribution of this paper (and how it differs from earlier methods) is the way the data are processed to estimate the length of a pile. Section 3 discusses the concept behind processing the data using the EDAR methodology.

3 Effective Dispersion Analysis of Reflections (EDAR): Theory

The fundamental concept of EDAR is based on the phase difference between the responses measured at the two sensor locations. The basic theory is explained for both longitudinal and flexural waves, followed by verification using synthetic data and validation using laboratory experiments. EDAR presents a unique way to process the same response data that can be obtained from the ultra-seismic or short kernel (bending wave) methods to estimate the length of the pile by incorporating the physical dispersion characteristics of wave propagation.

The phase difference between the responses at the two sensor locations in the frequency domain is given by,

$$P_d = \text{Imag}\left[\log\left(\frac{u_2(\omega)}{u_1(\omega)} \right) \right] \; , \tag{1}$$

where $u_1(\omega)$ and $u_2(\omega)$ are the Fourier transforms of the responses obtained at the two sensor locations, respectively. The phase difference between the responses obtained at the two sensor locations in the frequency domain contains the product of theoretical wavenumber (k) and the lengths associated with the structure. Generally, the phase depends on the distance the wave has traveled before and after reflections from the various boundaries in the structure. Section 3.1 explains the characteristics of the phase difference and extraction of the pile length using simple theoretical models: Section 3.1.1 discusses wave propagation without reflections and Section 3.1.2 discusses the effects of the reflections on an EDAR plot.

3.1   Longitudinal waves in bar

3.1.1   Propagation without reflections

Longitudinal or axial waves are nondispersive in nature and thus exhibit minimal variation in the initial waveform observed in the time domain. Figure 2 shows the simplest case of an infinite bar in which a propagating wave traveling from left to right is encountered once by the two sensors.
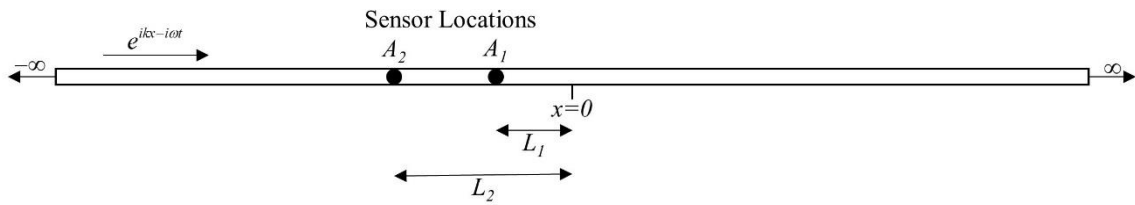

Figure 2: Schematic of infinite bar.

The second order differential equation describing the axial wave propagation in a rod is given by:

$$-EA\frac{\partial^2 u}{\partial x^2} + \rho A\frac{\partial^2 u}{\partial t^2} = 0 \; , \tag{2}$$

where E is Young's modulus, ρ is density, and A is area. The solution of the equation takes the form,

$$u = Ae^{ikx} \, , \tag{3}$$

where k is the wavenumber and ω is the temporal frequency. The wavenumber can be determined from the frequency by substituting Equation (3) into Equation (2), which gives the dispersion relation expressed as Equation (4).

$$k = \frac{\omega}{c_b} \, , \tag{4}$$

where c_b is the bar wave velocity and is given by $\sqrt{E/\rho}$. Substituting Equation **Error! Reference source not found.** in Equation (1) results in the phase difference:

$$P_d = k(L_2 - L_1) = k\Delta L \, . \tag{5}$$

Thus, the phase difference is a product of the theoretical wavenumber (k) and the distance between the sensors (ΔL). Practically, the phase difference that is calculated from the sensor responses results in wrapping between $-\pi$ and π.

An important aspect of this method is to plot the phase as a function of a newly defined quantity called the 'effective wavenumber' (k_e), which is a scaled wavenumber that does not require knowledge about material properties (or reduces the requirements for knowledge about material properties). In the specific case of a bar, because the theoretical wavenumber (k) in Equation (4) is directly proportional to the frequency, the effective wavenumber is simply defined as the frequency:

$$k_e^{bar} = \omega \, . \tag{6}$$

For reasons that will become clear after the reflections are analyzed in Section 3.1.2, the plot with the phase difference as the abscissa and the effective wavenumber as the ordinate is called the EDAR plot throughout the rest of the paper. The slope of the EDAR plot is governed by the distance between the sensors (ΔL) and the velocity of the wave propagation (c_b):

$$k_e^{bar} = \left(\frac{c_b}{\Delta L} \right) P_d \, . \tag{7}$$

The slope from equation (7) would determine the value on the effective wavenumber axis at which the phase gets wrapped. The value at which the first wrapping occurs is called the cycle period (K_I) and is given by

$$K_I^{bar} = \frac{\pi c_b}{\Delta L} \, . \tag{8}$$

 This is the first of the two periods associated with the phase and is a consequence of the initial arrival of the wave. Thus, the cycle is closely related to the time difference

11

between the initial arrivals of the propagating wave at the two sensor locations. As an example, consider a model bar of infinite length with a wave propagation velocity of 1 m/s and lengths $L_1 = 3m$ and $L_2 = 3.5m$, thus making the distance between the sensors $0.5m$. Figure 3 presents the EDAR plot that is obtained using the solution form in equation 3. The first wrapping of phase occurs at 2π, as is expected from Equation (8).

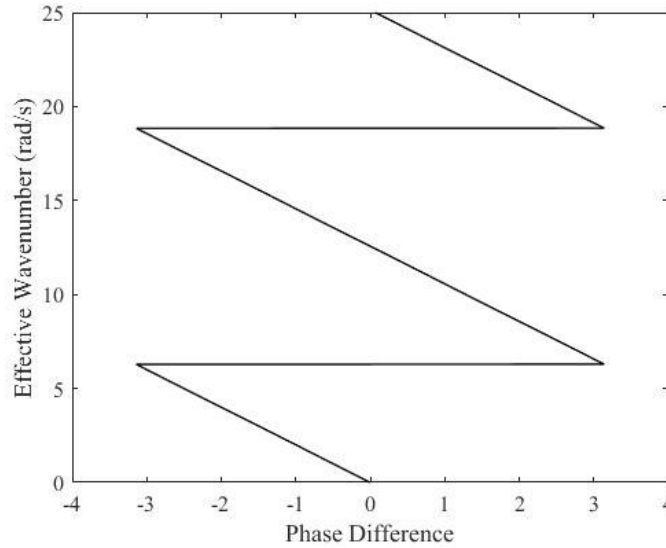**Figure 3:** EDAR plot for infinite bar: phase difference vs. effective wavenumber.

3.1.2 Effects of reflections on EDAR plot

Introducing a boundary at $x = 0$ makes the bar semi-infinite and results in a single reflection of the wave from the boundary; see Figure 4 that assumes a wave traveling from negative infinity towards the boundary where it gets reflected.
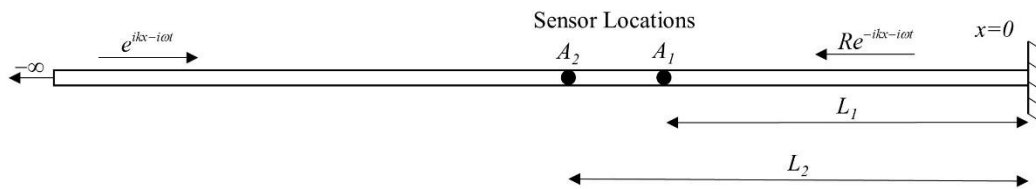

Figure 4: Semi-infinite bar: single reflection.

Without loss of generality, the displacement in the frequency domain anywhere in the bar can be assumed to be

$$u(x) = Ae^{ikx} + Be^{-ikx} ,$$

(9)

where the first term on the right-hand side represents a forward propagating wave and the second term represents the reflected wave. Similar to the infinite case, a model bar with the same parameters are considered for a semi-infinite bar, but the displacement form in equation (9) is used to account for the reflection from the boundary that is introduced; Figure 5 presents the resultant EDAR plot that is computed for a semi-infinite bar. In addition to the cycle oscillations that are similar to those found for the infinite bar, smaller oscillations can be observed with a smaller period in the semi-infinite bar. These small oscillations, called 'wiggles', are a consequence of the wave being reflected at the boundary and can be utilized to estimate the location of the boundary.
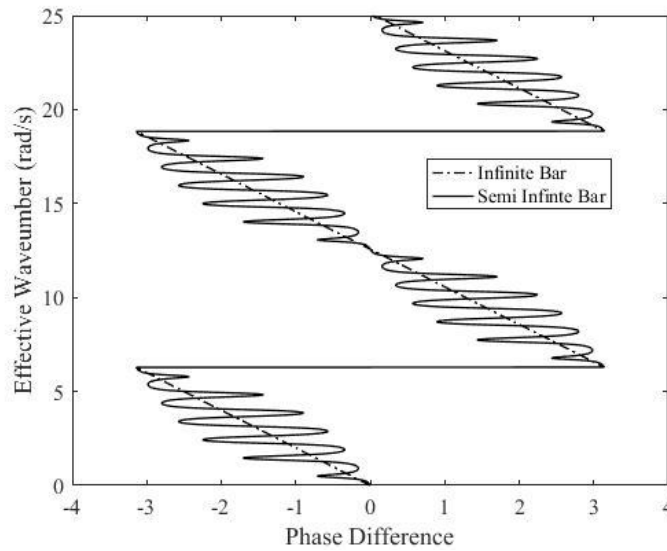

Figure 5: EDAR plot for semi-infinite bar superimposed on infinite bar.

The responses at the accelerometer locations A_1 and A_2 at distances L_1 and L_2, respectively, from the boundary are

$$u_1(L_1) = Ae^{ikL_1} + Be^{-ikL_1} ,$$

(10)

$$u_2(L_2) = Ae^{ikL_2} + Be^{-ikL_2} .$$

(11)

13

Using these displacements, the phase difference can be calculated from Equation (1). The steps involved in calculating the phase difference analytically are shown here as Equations (12) through (14).

$$\frac{u_1}{u_2} = \left(\frac{Ae^{2ikL_1} + B}{Ae^{2ikL_2} + B} \right) e^{ik(L_2 - L_1)} \tag{12}$$

Taking the logarithm of the ratio shown in Equation (12) gives

$$log\left(\frac{u_1}{u_2} \right) = ik(L_2 - L_1) + log(Ae^{2ikL_1} + B) - log(Ae^{2ikL_2} + B) \ . \tag{13}$$

The imaginary part of Equation (13) is the phase difference. The imaginary part of the logarithm of a complex number is the argument of the complex number and thus

$$P_d = \underbrace{k(L_2 - L_1)}_{b_1} + \underbrace{\tan^{-1}\left(\frac{A\sin(2kL_1)}{B + A\cos(2kL_1)} \right)}_{b_2} - \underbrace{\tan^{-1}\left(\frac{A\sin(2kL_2)}{B + A\cos(2kL_2)} \right)}_{b_3} \ . \tag{14}$$

The periodic nature of P_d can be explained from the three terms b_1, b_2, and b_3. The first term is exactly the same as the one obtained for the infinite bar and, along with phase wrapping, gives rise to the cycles shown in the EDAR plot in Figure 3. The terms b_2 and b_3 are responsible for the smaller oscillations or wiggles observed in Figure 5. The trigonometric functions b_2 and b_3 can be shown to have a period of π/L_1 and π/L_2, respectively. Because the distance between the sensors is small compared to the length of the pile [L_1 is approximately equal to L_2 that is approximately equal to L^e], L^e is the distance between the midpoints of the sensors to the boundary. Thus, the period of the last two terms in Equation (14) in the theoretical wavenumber (k) space is given by

$$K_R^{bar} = \frac{\pi c_b}{L} \ . \tag{15}$$

One of the main practical concerns here is obtaining an accurate estimate of the wave velocity for the system under consideration. Often, pile foundations are old and deteriorated and knowledge about the construction material is hard to obtain. Examining the ratio of the cycle and wiggle periods helps resolve this issue. The ratio of the cycle and wiggle periods is

$$\frac{K_I^{bar}}{K_R^{bar}} = \frac{\pi c_b / \Delta L}{\pi c_b / L^e} = \frac{L^e}{\Delta L} \ . \tag{16}$$

14

Once the cycle and wiggle periods are calculated from the EDAR plot, the only unknown is length L^e, which can be computed without need for any other information about the pile. Because the plot effectively captures (a) the effect of the dispersion relation (simple in this case but can be more complicated for beams) and (b) the effect of reflections from the boundary, the plot and the ensuing analysis that result in Equation (16) are referred to as the 'effective dispersion analysis of reflections', hence, 'EDAR'.

The proposed EDAR technique is similar to the travel-time approach for nondispersive systems, where the travel time between sensors can be used to compute the wave velocity, which in turn can be used to compute the unknown boundary locations based on the arrival times of the reflections. The key advantage of the proposed EDAR method is that it can be extended to dispersive wave propagation, where travel-time approaches fail due to the significant distortion of the waves that is caused by dispersion. Section 3.2 provides details regarding this extension of EDAR.

3.2   Flexural waves in beams

Bending waves can be generated by a lateral impact to the pile. The test set-up for bending waves is exactly the same as for longitudinal waves and the responses are likewise measured at a minimum of two sensor locations. There are two main differences between the waves propagating in a bar and a beam. Firstly, along with the propagating waves, there exists evanescent waves, which decay exponentially. Due to this decaying nature, the effect of evanescent waves on measured reflections is negligible and does not have a significant effect on EDAR processing. Secondly, the propagating waves are dispersive in nature as explained Equations (17) through (19) which is a critical for the formulation of the EDAR procedure.

The governing differential equation for a Bernoulli-Euler (BE) beam is given by

$$EI\frac{\partial^4 v}{\partial x^4} + \rho A \frac{\partial^2 v}{\partial t^2} = 0, \tag{17}$$

where v is the transverse displacement. Similar to the case for a bar, the general solution for Equation (17) can be given by

$$y = e^{ikx - i\omega t} \quad . \tag{18}$$

Substituting Equation (18) in Equation (17) we get the dispersion relation between wavenumber and temporal frequency given by

$$k = \sqrt{\frac{\omega}{c_b r}} \quad , \tag{19}$$

where c_b is the bar wave velocity and $r = \sqrt{I/A}$ is the radius of gyration. The phase and group velocities can be calculated from Equation (19); clearly, they are frequency-dependent, resulting in wave dispersion, which distorts the waveform as it propagates through the length of the beam. This wave distortion makes peak-picking difficult and often impossible, thus making travel-time approaches difficult.

The dispersion relation shown in Equation (19) is the key to defining the effective wavenumber for EDAR. The material constants and cross-sectional properties are dropped from the definition of the effective wavenumber for a BE beam in order to facilitate the estimation of length without prior knowledge about the constants, as indicated by Equation (20).

$$k_e^{BE} = \sqrt{\omega} \tag{20}$$

This particular definition makes the relation between the phase difference and effective wavenumber linear, and thus, all the expressions relating to EDAR obtained for a bar become applicable to a beam. The cycle and wiggle periods computed using the above definitions are

$$K_I^{BE} = \frac{\pi \sqrt{c_b r}}{\Delta L} \ , \tag{21}$$

$$K_R^{BE} = \frac{\pi \sqrt{c_b r}}{L^e} \ . \tag{22}$$

Similarly, taking the ratios of the two periods, a length estimate of the pile (L^e) can be obtained as

$$L^e = \frac{K_I^{BE} \Delta L}{K_R^{BE}} \ . \tag{23}$$

Once the responses at the sensor locations are obtained, Equation (23) requires only the cycle period, wiggle period, and the distance between the sensors to obtain an estimate for the length of the member. The important modification is the definition of the effective wavenumber as the square root of the frequency, thus making the wiggle period constant and facilitating the extension of the bar length estimation shown in Equation (16) to the beam length estimation shown in Equation (23).

This method pertains specifically to BE beam theory. BE beam theory is simple, but not accurate for higher frequencies where the wavelength is of the same order as the beam thickness. However, the EDAR methodology can be extended to more sophisticated models, such as Timoshenko beam theory. The governing equation for a Timoshenko beam with Young's modulus E, density ρ, shear modulus G, area A, moment of inertia I, and Timoshenko shear coefficient κ is

$$\frac{EI}{\rho A}\frac{\partial^4 y}{\partial x^4} - \left(\frac{I}{A} + \frac{EI}{GA\kappa}\right)\frac{\partial^4 y}{\partial x^2 \partial t^2} + \frac{\partial^2 y}{\partial t^2} + \frac{\rho I}{GA\kappa}\frac{\partial^4 y}{\partial t^4} = 0 \; . \tag{24}$$

The corresponding dispersion relation is

$$\frac{EI}{\rho A}k^4 - \left(\frac{I}{A} + \frac{EI}{GA\kappa}\right)\omega^2 k^2 - \omega^2 + \frac{\rho I}{GA\kappa}\omega^4 = 0 \; . \tag{25}$$

EDAR can be used with any model for which the dispersion relation can be obtained either theoretically (Timoshenko) or numerically (guided wave propagation). As models become more sophisticated, they more closely represent actual wave physics but at the same time lack the simplicity of the bar or BE beam model. Different material properties regarding structure might be needed as opposed to not requiring any material properties as is the case with the simpler BE beam model. The EDAR procedure must be used cautiously, paying utmost attention to the frequency content under consideration and the validity of the underlying models. At a lower frequency, use of BE beam theory might be justified, but at higher frequencies, more robust models, such as Timoshenko beam theory or even more sophisticated models based on guided wave theory, may be required.

3.3   Synthetic examples for EDAR verification

In this study, a finite BE beam was modeled with half spaces (HS) on the top and bottom with variable material properties to control the reflection coefficients and to treat reflections from different boundaries separately. Material damping was introduced by using complex values for the modulus of the pile. Table 1 presents the model BE beam properties and Figure 6 presents a schematic of the BE beam model with lengths.

Table 1: Model Bernoulli-Euler Beam Properties

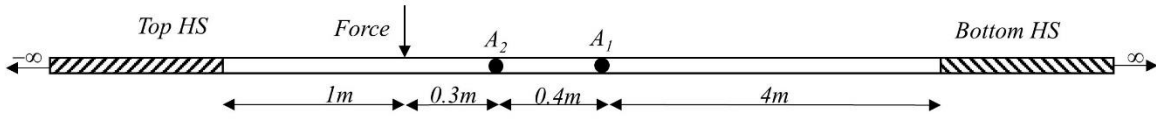| Property	Value
Young's Modulus	35 GPa
Density	2400 kg m/s^2
Poisson's Ratio	0.1

Figure 6: Schematic of Bernoulli-Euler beam model.

Example 1: The top HS is modeled such that it matches the beam to prevent reflections from the top. The bottom HS modulus is a large value to simulate a fixed end. Figure 7 presents the EDAR plot obtained from the BE model and Table 2 presents the BE model beam length estimates.
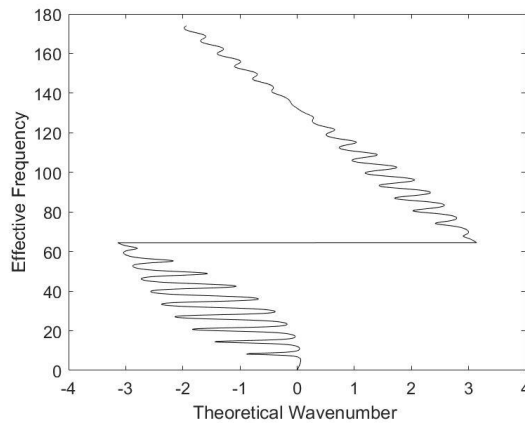

Figure 7: EDAR plot for synthetic Bernoulli-Euler beam experiment involving bottom reflections.

Table 2: Bernoulli-Euler Beam Model Length Estimate

Cycle Period	Wiggle Period	Distance between sensors	Estimated Length (m)	Actual Length (m)	Error
64.49	6.2	0.4	5.66	5.7	-0.7%

18

Example 2: Both the top and bottom HS moduli are set to a large value to simulate a beam with fixed boundary conditions on both ends. Figure 8 presents the EDAR plot obtained from the BE beam model.
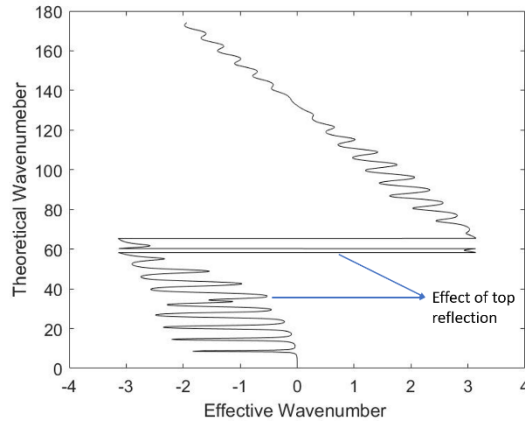

Figure 8: EDAR plot for Bernoulli-Euler beam model: bottom and top reflections.

Figure 8 shows the effect of the top reflection in the EDAR plot. Even though the top reflections disturbed the wiggle, the important aspect to note is the distinctive characteristics of the disturbances. They do not look similar to wiggles and can be ignored while calculating the wiggle period. This difference between the disturbances shown and wiggles is a consequence of the impact locations and the wave propagation direction. By using the wiggles in the EDAR plot, similar length estimates, as shown in Table 2, were obtained. Depending on the length to the top of the pile, there can sometimes be interference between the top effect and cycle frequency. This situation can be avoided by using multiple distances between the sensors, which we did during actual experimentation. We used four sensors instead of the two sensors required for EDAR. In this way, we built redundancy into the test and thus the cycle and wiggle periods can be obtained from multiple sensor combinations.

4 Experimental Validation of EDAR

Following the successful verification of EDAR using synthetic data, we performed experiments at the Constructed Facilities Laboratory at North Carolina State University (NCSU) to validate the proposed EDAR. Figure 9 shows one of the concrete filled steel tube (CFST) piles, installed as part of a different project at NCSU, which we used for initial testing. Table 3 presents the properties of the CFST.

Figure 9: Concrete filled steel tube tested at NCSU.

Table 3: Properties of Concrete Filled Steel Tube

Property	Value
Total Length	19 feet 5.25 inches
Embedded Length	13 feet 8 inches
Cap Dimensions	24 x 18 x 18 inches
Concrete Diameter	11.5 inches
Steel Thickness	0.25 inches

Accelerometers from PCB (352C33) and a data acquisition system from National Instruments (NI9232) were used respectively for sensing and recording the responses of CFST to a lateral impact from a small sledge-hammer. Figure 10 shows the equipment used for laboratory testing and Table 4 provides a summary of the equipment specifications.

Figure 10: Equipment used for EDAR testing.

Table 4: Equipment Specifications

Equipment type	Model	Important specifications	
		Item	Range
Accelerometer	PCB 352C33	Frequency	0 to 10000 Hz
		Measurement Range	±50 g
		Sensitivity	100 mV/g
DAQ System	NI 9234 with USB chassis	Analog Input Resolution	24 Bits
		Sampling Rate	51.2 KS/s

Four accelerometers were used to build redundancy in the data obtained, giving six two-sensor combinations. The distances between the four sensors were 8, 6, and 10 inches and are directly reflected in the cycle periods observed in the EDAR plots. Figure 11 presents the time domain plots of the accelerations obtained at the four sensor locations. Examining these time histories indicate that there are no clear peaks associated with incident and reflected waves, owing to the dispersion associated with flexural waves.
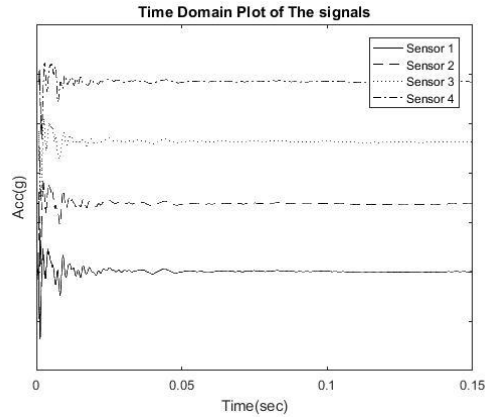
Figure 11: Experimental response: time domain

Figure 12 presents EDAR plots that clearly show the cycles and wiggles expected from the theory presented earlier in section 3. Raw data from the tests were processed using an exponential window in the time domain to reduce noise effects and to facilitate peak-picking to find the wiggle period.
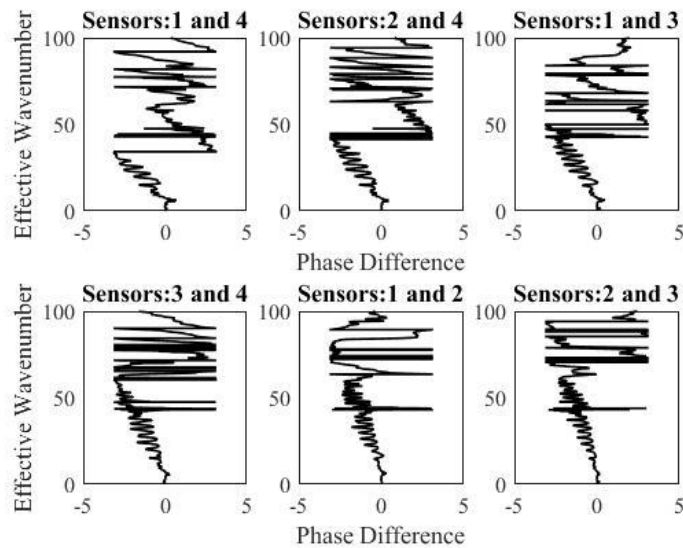

Figure 12: Representative experimental EDAR plots.

Figure 13 presents the theoretical dispersion relation computed based on the pile properties for BE and Timoshenko beam theories.
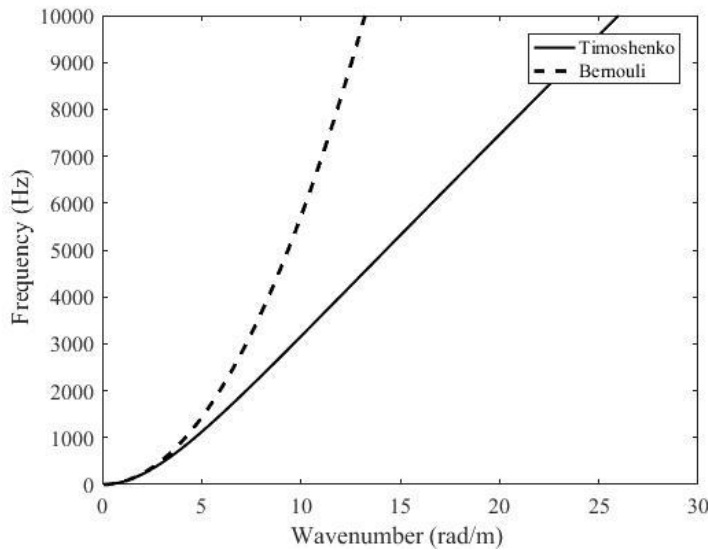
Figure 13: Theoretical dispersion relation: Bernoulli-Euler vs. Timoshenko beam theories.

It is well known that Timoshenko beam theory is more accurate than BE theory for higher frequencies, but at low frequencies the dispersion curves overlap for both models. Thus, using the lowermost wiggle in the frequency axis and cycle period between the farthest two sensors, a length estimate can be obtained.

Table 5: Length Estimate from First Observed Wiggle Using Bernoulli-Euler Beam Theory

Cycle period	Wiggle period from lowermost wiggle	Distance between sensors	Estimated length (m)	Actual length (m)	Error
34.18	3.63	.6096	18.83	19.42	3%

Even though the estimate presented in Table 5 is close to the actual length, with an error of 3 percent, many wiggles can be observed at different levels on the theoretical wavenumber axis. Each of these wiggles were used to calculate the wiggle period and subsequently used to estimate the length. As explained earlier, the main difference between the BE and Timoshenko beam theories is the theoretical wavenumber axis, and thus, the cycle and wiggle periods are changed, as shown in Figure 14. In Figure 15, the length estimates obtained from each observed wiggle are plotted as a function of the frequency at each wiggle. Clearly, the BE beam theory estimates are a function of the frequency and increase as we move up the frequency. This frequency dependence is reduced greatly for estimates obtained using Timoshenko beam theory, and the average error percentage also is reduced significantly (see Table 6).
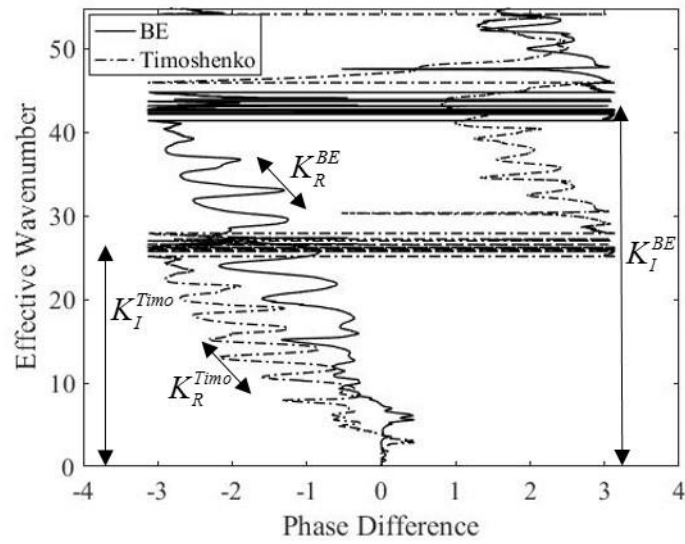
23

Figure 14: Comparison of Bernoulli-Euler and Timoshenko EDAR plots.
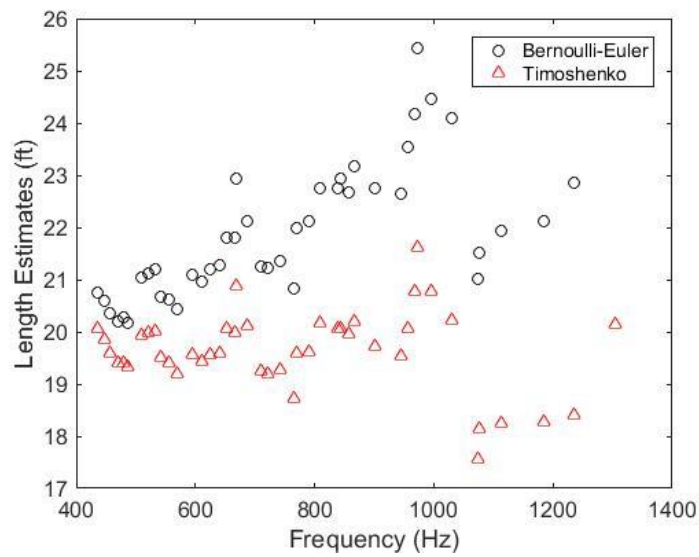

Figure 15: Length estimates as a function of frequency.

Table 6: Average Length Estimates

	Bernoulli-Euler theory	Timoshenko theory	Actual length (ft)
Estimate (ft)	21.94	19.65	19.42
Error	13%	1.18%	

24

Unlike Timoshenko beam theory, BE beam theory does not require any information about the pile properties to calculate the effective wavenumber defined in Equation (20). However, BE theory leads to a less accurate representation of the exact physical system, and thus, the resulting estimates are less accurate. Therefore, depending on the availability of material property estimates and location of the wiggles in the frequency axis, one of the two theories can be used to obtain the length. Note that only the relative value of shear stiffness compared to flexural stiffness is needed for Timoshenko beam theory; this value is often a function of Poisson's ratio, which tends not to change much.

In a more general sense, waves that propagate inside a pile are 'guided' waves owing to their three-dimensional nature and reflections from all the boundaries of the pile. Various research efforts conducted at Northwestern University by Finno [26], Hanifah [27], Chao [28], Wang [29], and Lynch [30] have considered the pile as a cylindrical wave guide to obtain the longitudinal, torsional, and flexural modes of vibrations and corresponding dispersion relation. The predominant modes in longitudinal and flexural waves are the first modes, namely L(0,1) and F(1,1), for frequencies excited via hammer impact, which gives us more confidence to use a 1-D wave propagation model.

Current and future work to improve the estimates at higher frequencies and potential improvements found in sophisticated models, such as those derived from guided wave theory, are being explored. The piles used in this study, despite being full scale, were relatively short in length compared to typical piles in the field. Also, the soil conditions for the tests were relatively loose soil, which could potentially have had a minimal effect on the EDAR estimations. Even though the methodology has been experimentally demonstrated to work for CFST piles, it should be applicable to other types of pile foundations as well. Such extension is left for future investigations.

5 Conclusion

A newly developed NDE methodology, EDAR, is introduced in this work. EDAR is based on obtaining the phase difference of responses at two different locations on a pile in the frequency domain as a function of a newly defined quantity called the 'effective wavenumber'. The effective wavenumber is a function of the dispersion relation of the model chosen to represent the physical system and the type of impact. The theory behind EDAR is based on longitudinal and flexural waves. We conducted experimental validation and found the pile length estimates to be consistently within a 5 percent error margin. EDAR methodology is based on the underlying physics of wave propagation and thus improves reliability for the results obtained. EDAR is currently being evaluated in the field, following its success in laboratory test conditions. Although we have demonstrated EDAR's effectiveness in estimating the length of a pile, the method should be extensible to other scenarios where the length of a member, e.g., an electricity pole, is to be determined.

Implementation and Technology Transfer Plan

A follow up project with NCDOT is currently underway which involves further field testing of the EDAR methodology. Avenues to explore are (a) hammer choice, (b) impact locations, (c) accelerometer spacing, (d) enhanced beam/waveguide theories, (e) investigation of the effect of the superstructure, and (f) effect of soil. These investigations require extensive field testing and advanced analysis (some field testing was conducted as part of this project and the results will be presented once the methodology is finalized as a part of the ongoing project). Furthermore, before the method can be routinely used in the field, blind validation must also be performed. Thus, a precise implementation plan is postponed until the completion of the ongoing project.

References

[1] L. D. Olson, F. Jalinoos, and M. F. Aouad, "Determination of Unknown Subsurface Bridge Foundations,(NCHRP 21-5 Interim Report Summary)," *Geotech. Eng. Noteb. Issuance GT-16. Fed. Highw. Adm. Washington, DC*, 1998.

[2] F. Rausche, "Non-Destructive Evaluation of Deep Foundations," 2004.

[3] S. Mclemore *et al.*, "Unknown Foundation Bridges Pilot Study," *Fed. Highw. Adm. Florida Dep. Transp.*, 2010.

[4] H. Wang and C.-H. Hu, "Identification on Unknown Bridge Foundations Using Geophysical Inspecting Methods," *e-Journal Nondestruct. Test.*, vol. 20(11), 90, 2015.

[5] Sarkar K.H., Islam M.S., Yasmin T., and Sarna S.A., "Determination of unknown bridge foundation depths with parallel seismic (PS) systems," 2015.

[6] J.-Y. Zhang, L.-Z. Chen, and J. Zhu, "Theoretical basis and numerical simulation of parallel seismic test for existing piles using flexural wave," *Soil Dyn. Earthq. Eng.*, vol. 84, pp. 13–21, 2016.

[7] J. T. Coe and B. Kermani, "Comparison of Borehole Ultrasound and borehole radar in evaluating the length of two unknown bridge foundations," *DFI J. - J. Deep Found. Inst.*, vol. 10, no. 1, pp. 8–24, Jan. 2016.

[8] K. F. Lo, S. H. Ni, Y. H. Huang, and X. M. Zhou, "Measurement of unknown bridge foundation depth by parallel seismic method," *Exp. Tech.*, vol. 33, no. 1, pp. 23–27, 2009.

[9] E. J. Mercado and M. W. O'Neill, "Methods to measure scour depth and the depth of unknown foundations," *3rd Int. Conf. Appl. Geophys.*, 2003.

[10] D. A. Sack, S. H. Slaughter, and L. D. Olson, "Combined Measurement of Unknown Foundation Depths and Soil Properties with Nondestructive Evaluation Methods," *Transp. Res. Rec. J. Transp. Res. Board*, no. 1868, pp. 76–80, 2004.

[11] J. F. Levy, "Sonic pulse method of testing Cast-in-Situ concrete piles," *Gr. Eng.*, vol. 3, p. 17–19., 1970.

[12] A. G. Davis, C. S. Dunn, and CEBTP., "From Theory to Field Experience with the Non-Destructive Vibration Testing of Piles.," *Proceedings of the Institution of Civil Engineers*, vol. 57, no. 4. pp. 571–593, 1974.

[13] F. Rausche, G. G. Goble, and G. E. Likins, "Dynamic Determination of Pile Capacity," *J. Geotech. Eng.*, vol. 111, no. 3, pp. 367–383, 1985.

[14] H. F. C. Chan, "Non-destructive testing of concrete piles using the sonic echo and transient shock methods," 1987.

[15] Y. Lin, M. Sansalone, and N. J. Carino, "Impact-Echo Response of Concrete Shafts," *Geotech. Test. Journal, GTJODJ*, vol. 14, no. 2, pp. 121–137, 1991.

[16] M. Hussein, W. Wright, and B. Edge, "Low Strain Dynamic Testing of Wood Piles Supporting an Existing Pier," *Struct. Congr. XII*, pp. 940–945, 1994.

[17] A. G. Davis, "Nondestructive Evaluation of Existing Deep Foundations," *J. Perform. Constr. Facil.*, vol. 9, no. 1, pp. 57–74, 1995.

[18] J.-L. Briaud, J.-L. Briaud, M. Ballouz, G. Nasr, and S. J. Buchanan, "Defect And Length Predictions By NDT Methods For Nine Bored Piles," *Deep Found. 2002 An Int. Perspect. Theory, Des. Constr. Perform.*, pp. 173–192, 2002.

[19] B. Jozi, U. Dackermann, R. Braun, J. Li, and B. Samali, "Application and improvement of conventional stress-wave-based non-destructive testing methods for the condition assessment of in-service timber utility poles," *Australas. Conf. Mech. Struct. Mater.*, pp. 9–12, 2014.

[20] S. Rashidyan, "Characterization of Unknown Bridge Foundations," *Dr. Diss. Univ. New Mex.*, 2017.

[21] M. S. Hossain, ; M S Khan, J. Hossain, G. Kibria, and T. Taufiq, "Evaluation of Unknown Foundation Depth Using Different NDT Methods," *J. Perform. Constr. Facil.*, vol. 27, no. 2, pp. 209–214, 2011.

[22] R. A. Douglas and J. D. Holt, "Determining length of installed timber pilings by dispersive wave propagation methods," 1994.

[23] M. Subhani, J. Li, B. Samali, and N. Yan, "Determination of the embedded lengths of electricity timber poles utilizing flexural wave generated from impacts," *Aust. J. Struct. Eng.*, vol. 14, no. 1, pp. 85–96, 2013.

[24] A. T. M. Farid, "Prediction of unknown deep foundation lengths using the Hilbert Huang Transform (HHT)," *HBRC J.*, vol. 8, no. 2, pp. 123–131, 2012.

[25] S.-H. Ni, J.-L. Li, Y.-Z. Yang, and Z.-T. Yang, "An improved approach to evaluating pile length using complex continuous wavelet transform analysis," *Insight - Non-Destructive Test. Cond. Monit.*, vol. 59, no. 6, pp. 318–324, 2017.

[26] R. J. Finno, "1-D Wave Propagation Techniques in Foundation Engineering," in *Art of Foundation Engineering Practice*, 2010, pp. 260–277.

[27] A. Hanifah, "A theoretical evaluation of guided waves in deep foundations.," *Northwest. Univ.*, 2000.

[28] H. C. Chao, "An Experimental Model for Pile Integrity Evaluation using a Guided Wave Approach," *Northwest. Univ.*, 2002.

[29] H. Wang, "Theoretical Evaluation of Embedded Plate-Like and Solid Cylindrical Concrete Structures with Guided Waves," *Northwest. Univ.*, 2004.

[30] J. J. Lynch, "Experimental verification of flexural guided waves in concrete cylindrical piles," *Northwest. Univ.*, 2007.